

# X-ray/UV/Optical follow-up of the blazar PKS 2155–304 after the giant TeV flares of July 2006

L. Foschini<sup>1,\*</sup>, G. Ghisellini<sup>2</sup>, F. Tavecchio<sup>2</sup>, A. Treves<sup>3</sup>, L. Maraschi<sup>2</sup>, M. Gliozzi<sup>4</sup>, C.M. Raiteri<sup>5</sup>, M. Villata<sup>5</sup>, E. Pian<sup>6</sup>, G. Tagliaferri<sup>2</sup>, G. Tosti<sup>7</sup>, R.M. Sambruna<sup>8</sup>, G. Malaguti<sup>1</sup>, G. Di Cocco<sup>1</sup>, P. Giommi<sup>9</sup>

## ABSTRACT

We present all the publicly available data, from optical/UV wavelengths (UVOT) to X-rays (XRT, BAT), obtained from *Swift* observations of the blazar PKS 2155–304, performed in response to the rapid alert sent out after the strong TeV activity (up to 17 Crab flux level at  $E > 200$  GeV) at the end of July 2006. The X-ray flux increased by a factor of 5 in the 0.3 – 10 keV energy band and by a factor of 1.5 at optical/UV wavelengths, with roughly one day of delay. The comparison of the spectral energy distribution built with data quasi-simultaneous to the TeV detections shows an increase of the overall normalization with respect to archival data, but only a small shift of the frequency of the synchrotron peak that remains consistent with the values reported in past observations when the TeV activity was much weaker.

*Subject headings:* BL Lacertae objects: general – BL Lacertae objects: individual: PKS 2155-304

---

<sup>1</sup>INAF/IASF-Bologna, Via Gobetti 101, 40129 Bologna (Italy)

<sup>2</sup>INAF/Osservatorio Astronomico di Brera, Via Brera 28, 20121 Milano (Italy)

<sup>3</sup>Dipartimento di Scienze, Università dell’Insubria, Via Vallegio 11, 22100 Como (Italy)

<sup>4</sup>George Mason University, Department of Physics and Astronomy, School of Computational Sciences, Mail Stop 3F3, 4400 University Drive, Fairfax, VA 22030, USA

<sup>5</sup>INAF/Osservatorio Astronomico di Torino, Via Osservatorio 20, 10025 Pino Torinese (Italy)

<sup>6</sup>INAF/Osservatorio Astronomico di Trieste, Via G.B. Tiepolo 11, 34131 Trieste (Italy)

<sup>7</sup>Osservatorio Astronomico, Università di Perugia, Via B. Bonfigli, 06126 Perugia (Italy)

<sup>8</sup>NASA/Goddard Space Flight Center, Code 661, Greenbelt, MD 20771, USA

<sup>9</sup>ASI Science Data Centre, Via G. Galilei, 00044 Frascati, (Italy)

\*Email: foschini@iasfbo.inaf.it

## 1. Introduction

PKS 2155–304 ( $z = 0.116$ ) is one of the best known blazars and the second brightest in X-rays (after Mkn 421), observed many times at various wavelengths. At  $\gamma$ -ray energies, it was first detected by CGRO/EGRET with a photon index  $\Gamma = 1.71 \pm 0.24$  in the energy range 0.03 – 10 GeV (Vestrand et al. 1995). This hard spectrum suggested a possible detection in the TeV energy range (Vestrand et al. 1995, Stecker et al. 1996, Tavecchio et al. 1998) that was first achieved by the University of Durham Mark 6 Čerenkov telescope in 1996 – 1997 (Chadwick et al. 1999).

In 2002–2003 the TeV activity has been monitored by HESS<sup>1</sup> that detected a flux variation in the  $E > 300$  GeV energy band from 1.2 to  $7.8 \times 10^{-11}$  ph cm<sup>-2</sup> s<sup>-1</sup> equivalent to 90 – 560 mCrab (Aharonian et al. 2005a). At the end of July 2006, the source displayed an anomalously high activity. Preliminary analysis of the HESS data showed an average flux level of 8 Crab in the  $E > 200$  GeV energy band with flares up to 17 Crab during the night of 27 – 28 July, an average flux level of 1 Crab during the night of 28 – 29 July with smaller activity, while a second outburst occurred in the night of 29 – 30 July with an average of 5 Crab and flares up to 13 Crab (Raue et al. 2006, Aharonian et al., in prep.). The event was detected also by MAGIC<sup>2</sup> (A. De Angelis, private communication). Following a rapid alert (Benbow et al. 2006) some high-energy satellites pointed at PKS 2155–304.

The *Swift* satellite (Gehrels et al. 2004) performed optical/UV and X-ray follow-up, starting on July 29 ending on August 29 2006, with repeated short exposure pointings. Here we present the results of these observations, a comparison with previous ones, when PKS 2155–304 was in a low activity state and theoretical modeling of the SEDs.

## 2. Data analysis

The data from the three instruments onboard *Swift* have been processed and analyzed with HEASoft v. 6.1.2 with the latest calibration files (6 December 2006).

Data from individual pointings from the coded-mask hard X-rays detector BAT (optimized for the 15 – 150 keV energy band, Barthelmy et al. 2005) were binned, cleaned from hot pixels and background, and deconvolved. The intensity images were then integrated by using the variance as weighting factor. PKS 2155–304 was not detected either in individual

---

<sup>1</sup><http://www.mpi-hd.mpg.de/hfm/HESS/>

<sup>2</sup><http://wwwmagic.mppmu.mpg.de/>

pointings nor in the integrated mosaic image. The upper limit for a  $3\sigma$  detection in the 20 – 40 keV energy band – already corrected for systematics – is  $3.3 \times 10^{-10}$  erg cm $^{-2}$  s $^{-1}$  (42 mCrab) for the pointing of 29 July 2006 (exposure 6 ks) and  $1.6 \times 10^{-10}$  erg cm $^{-2}$  s $^{-1}$  (20 mCrab) for the overall mosaic (exposure 30 ks).

Data from the X-ray Telescope XRT (0.3 – 10 keV, Burrows et al. 2005) were analyzed using the `xrtpipeline` task. XRT automatically switches the operating mode according to the target source flux, changing from window timing (WT, high flux) to photon counting (PC, low flux) with a threshold around 1 mCrab ( $5 \times 10^{-11}$  erg cm $^{-2}$  s $^{-1}$ ). The X-ray flux of PKS 2155–304 remained almost always above  $\approx 10^{-10}$  erg cm $^{-2}$  s $^{-1}$  (Fig. 1) and therefore we analyzed only the window timing mode data. There are also a few hundreds of seconds exposure in photon counting mode, but the point-spread function (PSF) is severely affected by pile-up. Nevertheless, we used the source position measured in the images accumulated with PC data as best input for the pipeline of WT mode (without imaging). We selected only the grade 0 (single pixel) events and extracted the spectra only from pointings with exposures greater than 100 s, in order to have the best available statistics. The remaining pointings (i.e. with less than 100 s) are anyway included in the lightcurve displayed in the top panel of Fig. 1, in order to give a better coverage of the time evolution of the source.

Since most of the pointings lasted a few hundreds of seconds, there exposure is insufficient to have data at energies above 4 – 6 keV, except for the pointing of 29 July, where a 5 ks exposure allowed us to have useful signal up to 8 keV. In addition, the XRT response is limited at low energies, because there are still some residual instrumental feature around 0.5 keV (Campana et al. 2006). Therefore, the extracted spectra were fitted in the range 0.3 – 0.45 keV and from 0.6 to 4 – 8 keV, depending on the statistics and then the flux was measured in the full 0.3 – 10 keV band. The results are summarized in Table 1.

For XRT, we note that the observation indicated in Table 1 as “29/31-07” actually started on 29 July 2006 at 00 : 55 : 42 UTC and ended on 31 July 2006 at 00 : 01 : 00 UTC, resulting in an elapsed time of  $\approx 1.7 \times 10^5$  s. However, the effective exposure time is only 4916 s. Thus, the spectral data reported in Table 1 refer to the average of the snapshot observations during this period. In addition, we also extracted from this observation, the subset of data referring only to the night between 29 and 30 July, in order study the data available that are simultaneous to TeV observations. The spectral information about that night are indicated in Table 1 as “30-07”.

Data from the optical/UV telescope UVOT (Roming et al. 2005) were analyzed by using the `uvotmagnhist` task with a source region of 6'' for optical and 12'' for UV filters. The background was extracted from an annular region centered on the source and with an inner region equal to the source region plus 2'' and the outer radius equal to 60''. To take into

account systematic effects, we added a 10% error in flux (resulting in about 0.1 magnitudes). The results, simultaneous to the X-ray fits, are summarized in Table 1, while complete lightcurves are shown in Fig. 1.

In order to compare X-rays/UV/optical data close to the outburst with data when PKS 2155–304 was not active (i.e. with low X-ray/UV/optical fluxes), we retrieved and analyzed *Swift* observations of the blazar performed in April 2006. The results of the analysis are reported in Table 1 where the flux difference between April and August observations shows up clearly.

### 3. Discussion and interpretation

#### 3.1. Overview of data

The *Swift* observations of PKS 2155 – 304 starting on July 29th at 00 : 55 during the phase of strong TeV activity reported by HESS (Raue et al. 2006, Aharonian et al., in prep.), show an initial increase of the X-ray flux, by a factor 4, between the observation of 29 July and that of 30 July followed by an overall decrease, while optical/UV fluxes show a moderate activity (Fig. 2). No detection in hard X-rays was obtained with BAT.

With respect to the April 2006 observations, XRT recorded a change by a factor 5, while the UV flux increased by a factor of  $\approx 1.5$ . For comparison the HESS observations of July 2006 showed "night-averaged" intensities in the TeV band of factors  $\approx 16$  and  $\approx 10$  larger than those in 2002 – 2003 (0.5 Crab; Aharonian et al. 2005), but with short flares of up to a factor of 34.

The sparseness of the available data does not allow us to make stringent correlations with TeV data. We note however that the initial flare in X-rays taking place between the nights of 29 and 30 July, approximately coincides with the second TeV outburst, while a lower amplitude flare in the UV occurs about one day later (Fig. 2). Since the UVOT detector often saturated because of coincidence losses, we cannot exclude the occurrence of other flares with greater amplitude.

#### 3.2. Spectral Energy Distribution

With the current data set we cannot probe the short (5 min) timescale variability preliminarily reported by HESS (Raue et al. 2006; Aharonian et al., in prep.), but can investigate only quantities averaged over timescales of days. We therefore assembled the

spectral energy distribution (SED, Fig. 3) using the *Swift* observation tagged as “30 July” that is quasi-simultaneous to the second TeV flare occurred during the night between 29 – 30 July 2006. We also considered TeV and *Swift* observations performed on 2 August, when the blazar activity was declining.

In order to discuss the observed SEDs in terms of changes of relevant physical quantities, we used the model by Ghisellini et al. (2002) to reproduce the SEDs in Fig. 3. As generally assumed for this and the other TeV BL Lacs (e.g. Aharonian 2004) the X-ray emission is attributed to synchrotron radiation and the  $\gamma$ -ray component to the synchrotron self-Compton (SSC) process. The source is assumed to be a sphere of radius  $R$  travelling with bulk Lorentz factor  $\Gamma$  at an angle  $\theta$  with respect to the line of sight, yielding a Doppler factor  $\delta$ . The magnetic field  $B$  is tangled and homogeneous. The distribution of emitting relativistic electrons is computed as the result of a broken power law injection distribution  $\propto \gamma^{-s}$  between  $\gamma_1$  and  $\gamma_2$ , and  $\propto \gamma^{-1}$  below  $\gamma_1$ , subject to radiative cooling occurring in a light crossing time  $R/c$ . This injection of relativistic particles correspond to an injected power  $L'_{\text{inj}}$  as measured in the comoving frame. The resulting particle distribution  $N(\gamma)$  is formed by power law segments, the steepest of which is  $\propto \gamma^{-(s+1)}$ . All the parameters corresponding to the two models shown in Fig. 3 are listed in Table 2. Tavecchio et al. (1998) have shown that, in principle, if the peak frequencies and fluxes of the synchrotron and self-Compton components and the variability timescales are known, then the main parameters for the SSC model are determined. At present we have only a very partial knowledge of the SED at high energies, resulting in ambiguities in the parameter choice. To fix them, we minimized the luminosity in the self-Compton component assuming an intrinsically steep TeV spectrum. We have also assumed that the variability timescales is  $\sim 1$  hour, as typically observed in the X-ray band (e.g. Zhang et al. 2002). The much shorter 5 minute variability timescale recently observed in the TeV band should then imply a different additional region/emission process.

The model results show that, while there is some evidence of a flatter X-ray spectrum at higher intensity, the frequency of the synchrotron peak remains at  $\approx 10^{15-16}$  Hz, consistent with other observations with much weaker TeV activity (cf Urry et al. 1997, Chiappetti et al. 1999, Foschini et al. 2006). The low peak frequency value is also a result of the choice of reproducing the optical-UV fluxes. The large difference in TeV fluxes associated with small differences in X-ray spectra requires, in SSC models, an increase of the relativistic electrons accompanied by a decrease of the magnetic field.

The above point is confirmed by a comparison of the present data and model with the *BeppoSAX* observation in November 1997 (Chiappetti et al. 1999) which was performed quasi-simultaneously to the TeV observations by Chadwick et al. (1999), when PKS 2155–

304 was at about 0.3 Crab (average flux,  $E > 300$  GeV). With respect to the parameters derived for the November 1997 episode the present SSC models yield (cf. Table 2) a larger Doppler factor ( $\delta = 33$  vs 18), a smaller magnetic field ( $B = 0.27\text{--}0.55$  G vs 1 G), a flatter index of the electron distribution ( $p = s + 1 = 3.5\text{--}3.6$  vs 4.85), and a smaller frequency of the synchrotron peak ( $\approx 10^{16}$  vs  $10^{17}$  Hz) with very similar emitting regions ( $R = 5 \times 10^{15}$  vs  $3 \times 10^{15}$  cm).

In summary, within a simple SSC scheme, the physical parameters of the source changed, in the sense of a harder particle spectrum, a smaller magnetic field and a greater beaming factor in the 2006 observations. This is required by the the different self-Compton to synchrotron luminosity ratio, which was substantially larger in the 2006 observations.

### 3.3. Comparison with other cases: Mkn 501 in 1997, Mkn 421 1998-2000

It is interesting to compare the present episode with other exceptional activity states occurred in the past in blazar sources with similar SEDs (HBL, Padovani & Giommi 1995). The most striking example to date is the strong TeV activity exhibited by Mkn 501 in April 1997, observed by the Whipple Observatory: during the nights from 7 to 19 April 1997, its flux ( $E > 350$  GeV) changed from 0.5 to the peak of 3.8 Crab occurred on 16 April, with an average of 1.6 Crab and no hourly timescale variability (Catanese et al. 1997). *BeppoSAX* observed the simultaneous highly chromatic evolution of the source in X-rays: the flux increased by factors of 4.2, 2.4, and 1.5 in the 13 – 200 keV, 2 – 10 keV, and 0.1 – 2 keV energy bands respectively, resulting in a frequency shift of the synchrotron peak by two orders of magnitude (Pian et al. 1998, Tavecchio et al. 2001). RXTE observations revealed also timescales variability down to a few tens of minutes (Xue & Cui 2005). Observations with U filter showed a modest increase of 1% in flux (Catanese et al. 1997). A less extreme, though analogous, behaviour was observed in Mkn 421 in 1998-2000. The X-ray and TeV activity were correlated also on short timescale (Maraschi et al 1999, Takahashi et al. 2000) with larger amplitude variations in the TeV band. The synchrotron peak appeared to shift to higher energies but not as dramatically as for Mkn 501.

The behaviour of PKS 2155-304 appears less striking in X-rays than for the previous two sources but more extreme in the TeV variability. The important questions to be answered concern the understanding of these different "modes" of variability in terms of physical models of the sources. The upcoming gamma-ray missions (AGILE -GLAST) and the continuous developments of Cherenkov Telescope facilities will allow to define the spectral variability at high energies with unprecedented accuracy. It is however mandatory to complement the high energy data with extensive observations in the X-ray band in order to approach the

physical origin of the variability.

#### 4. Conclusions

We presented the observations of the blazar PKS 2155–304 performed by the *Swift* satellite immediately after the giant TeV flare observed by HESS at the end of July 2006 (Raue et al. 2006; Aharonian et al., in prep.). The most important result appears to be that, in correspondence with the dramatic TeV activity, the X-ray intensity changed by a factor 5 but without large spectral changes. In particular the frequency of the synchrotron peak remained at values similar to those observed in the past (e.g. 1997, Chiappetti et al. 1999), during low TeV activity. Modeling of the SED based on the SSC process in a homogeneous region suggests an increase of the Doppler factor (33 in 2006; 18 in 1997) and of the relativistic electrons associated with a decrease of the magnetic field (0.27 G in 2006; 1 G in 1997).

LF thanks V. Bianchin for useful discussions. This research has made use of data obtained from the High Energy Astrophysics Science Archive Research Center (HEASARC), provided by NASA’s Goddard Space Flight Center.

#### REFERENCES

- Aharonian F., Akhperjanian A.G., Aye K.-M., et al., 2005a, A&A 430, 865
- Aharonian F., Akhperjanian A.G., Aye K.-M., et al., 2005b, A&A 442, 895
- Aharonian, F. A. 2004, Very high energy cosmic gamma radiation : a crucial window on the extreme Universe, by F.A. Aharonian. River Edge, NJ: World Scientific Publishing, 2004
- Barthelmy S.D., Barbier L.M., Cummings J.R., et al., 2005, Space Sci. Rev. 120, 143
- Benbow W., Costamante L., Giebels B. on behalf of the HESS Collaboration, 2006, ATel 867
- Burrows D.N., Hill J.E., Nousek J.A., et al., 2005, Space Sci. Rev. 120, 165
- Campana S., Beardmore A.P., Cusumano G., Godet O., 2006, Swift XRT CALDB Release Note 09: Response matrices and Ancillary Response Files

- Catanese M., Bradbury S.M., Breslin A.C., et al., 1997, ApJ 487, L143
- Chadwick P.M., Lyons K., T.J.L. McComb, et al., 1999, ApJ 513, 161
- Chiappetti L., Maraschi L., Tavecchio F., et al., 1999, ApJ 521, 552
- Foschini L., Ghisellini G., Raiteri C.M., et al., 2006, A&A 453, 829
- Gehrels N., Chincarini G., Giommi P., et al., 2004, ApJ 611, 1005
- Ghisellini G., Celotti A., Costamante L., 2002, A&A 386, 833
- Kataoka J., Takahashi T., Wagner S.J., et al., 2001, ApJ 560, 659
- Lockman F.J., Savage B.D., 1995, ApJSS 97, 1
- Maraschi, L., et al. 1999, ApJ, 526, L81
- Padovani P. & Giommi P., 1995, ApJ 444, 567
- Pian E., Vacanti G., Tagliaferri G., et al., 1998, ApJ 492, L17
- Raue M. on behalf of the HESS Collaboration, 2006, In: The keV to TeV Connection. Roma, 17-19 October 2006 [[http://gri.rm.iasf.cnr.it/keVtoTeV/Docs\33\\_Mraue.pdf](http://gri.rm.iasf.cnr.it/keVtoTeV/Docs\33_Mraue.pdf)]
- Roming P.W.A., Kennedy T.E., Mason K.O., et al., 2005, Space Sci. Rev. 120, 95
- Stecker F.W., de Jager O.C., & Salamon M.H., 1996, ApJ 473, L75
- Stecker F.W. & Scully S.T., 2006, ApJ 652, L9
- Takahashi, T., et al. 2000, ApJ, 542, L105
- Tanihata C., Urry C.M., Takahashi T., et al., 2001, ApJ 563, 569
- Tavecchio F., Maraschi L., & Ghisellini G., 1998, ApJ 509, 608
- Tavecchio F., Maraschi L., Pian E., et al., 2001, ApJ 554, 725
- Urry C.M., Treves A., Maraschi L., et al., 1997, ApJ 486, 799
- Vestrand W.T., Stacy J.G., & Sreekumar P., 1995, ApJ 454, L93
- Xue Y. & Cui W., 2005, ApJ 622, 160
- Zhang, Y.H., Treves, A., Celotti, A. et al., 2002, ApJ, 572, 762



Table 1. Summary for Swift observations. See Fig. 1 for the complete set of data.

Date	XRT Exposure [s]	Parameters <sup>a</sup>	F <sup>b</sup>	$\chi^2/\text{dof}$	V <sup>c</sup>	B <sup>c</sup>	U <sup>c</sup>	UVW1 <sup>c</sup>	UVM2 <sup>c</sup>	UVW2 <sup>c</sup>
<i>April 2006</i>										
16 – 04	400	$2.40 \pm 0.09$	0.94	1.36/41	13.0	13.4	12.5	12.3	12.6	12.6
26 – 04	155	$2.4 \pm 0.1$	1.31	0.99/20	12.8	13.2	12.3	12.0	12.4	12.3
<i>July-August 2006</i>										
29/31 – 07	4916	$2.30 \pm 0.03, 1.19^{+0.09}_{-0.11}, 2.80 \pm 0.04$	3.43	1.22/319	12.6	13.0	12.1	11.7	12.0	11.9
30/07	3276	$2.25 \pm 0.03, 1.2 \pm 0.1, 2.81 \pm 0.05$	3.61	1.17/287						
01 – 08	351	$2.62 \pm 0.05$	2.90	1.17/93	12.5	< 12.8	< 12.0	< 11.3	11.7	11.7
02 – 08	1842	$2.44^{+0.05}_{-0.07}, 1.2 \pm 0.2, 2.90^{+0.10}_{-0.08}$	2.46	1.06/195	12.5	12.9	< 12.0	11.4	11.8	11.7
03 – 08	1605	$2.24^{+0.05}_{-0.13}, 1.1^{+0.1}_{-0.2}, 2.75^{+0.06}_{-0.08}$	2.96	1.31/205	12.6	12.9	< 12.0	11.6	11.9	11.9
05 – 08	517	$2.67 \pm 0.05$	2.01	0.96/93	12.6	13.0	< 12.0	11.6	11.9	11.8
06 – 08	295	$2.64 \pm 0.08$	1.68	0.91/52	12.7	13.0	–	11.6	–	–
08 – 08	439	$2.62 \pm 0.05$	2.29	0.93/91	–	–	–	–	–	–
10 – 08	318	$2.58 \pm 0.06$	2.17	0.91/70	12.6	12.9	< 12.0	< 11.3	11.8	11.7
12 – 08	139	$2.8 \pm 0.2$	1.27	1.10/17	12.5	12.8	< 12.0	< 11.3	12.2	11.6
20 – 08	184	$2.4 \pm 0.1$	1.14	1.09/25	12.5	12.9	< 12.0	11.6	11.9	11.8
22 – 08	161	$2.6 \pm 0.1$	1.62	1.42/25	12.5	12.9	< 12.0	11.5	11.9	11.8

<sup>a</sup> $\Gamma$  for the power law model or  $\Gamma_1, E_{\text{break}}$  [keV],  $\Gamma_2$ , respectively, for the broken power law model. The absorption column is fixed to the Galactic value ( $N_{\text{H}} = 1.36 \times 10^{20} \text{ cm}^{-2}$ , Lockman & Savage 1995).

<sup>b</sup>Observed flux in the 0.3 – 10 keV band [ $10^{-10} \times \text{erg cm}^{-2} \text{ s}^{-1}$ ].

<sup>c</sup>Observed magnitudes. Error 0.1 mag for all, including systematics. Lower limits indicate a saturation of the detector.

Table 2: Parameters for the SSC model by Ghisellini, Celotti & Costamante (2002) used to interpolate the SED (Fig. 3).  $\Gamma_{\text{bulk}}$  is the bulk Lorentz factor,  $\theta$  the viewing angle,  $\delta$  the Doppler factor, and  $B$  the magnetic field. See the text for more details.

	Jul 29	Aug 2	Units
$R$	5	5	$10^{15}$ cm
$L'_{\text{inj}}$	1.1	0.3	$10^{42}$ erg s $^{-1}$
$\gamma_{\text{break}}$	1.5	0.9	$10^4$
$\gamma_{\text{max}}$	1.75	1.1	$10^5$
$s$	2.5	2.6	
$B$	0.27	0.55	Gauss
$\Gamma_{\text{bulk}}$	30	30	
$\theta$	1.7	1.7	degrees
$\delta$	33.5	33.5	

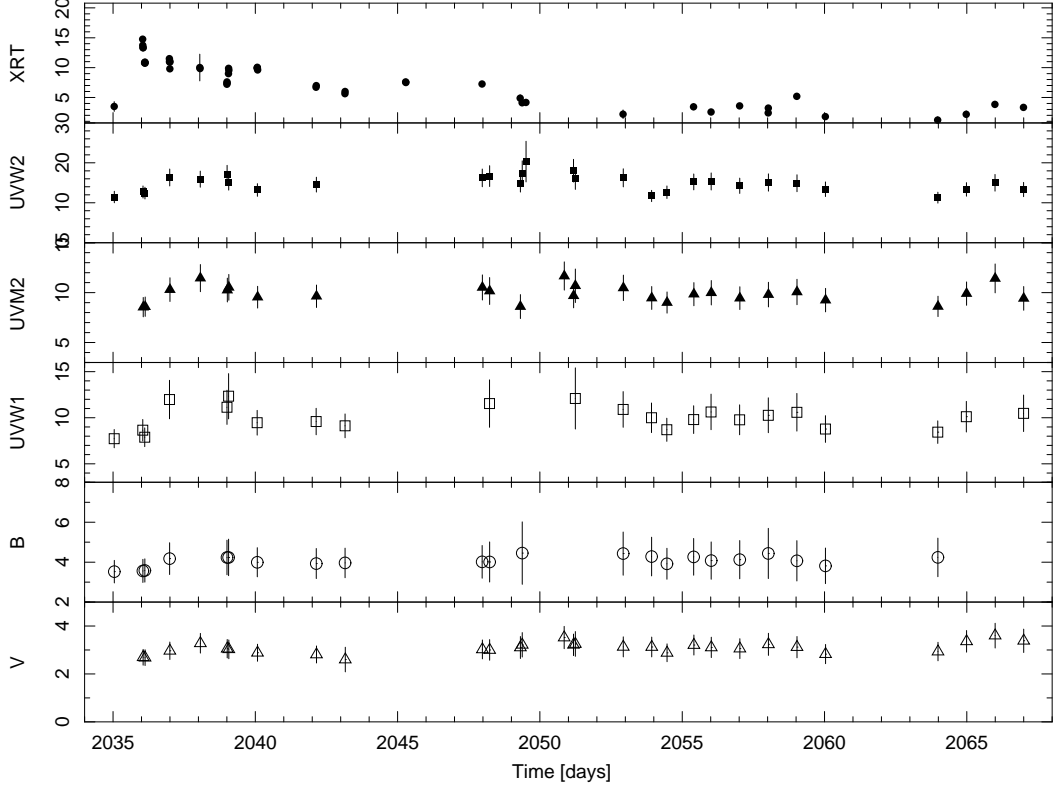


Fig. 1.— Lightcurves built from data of *Swift* instruments. From top to bottom: XRT [0.3 – 10 keV], UVOT UVW2 (1880 Å), UVM2 (2170 Å), UVW1 (2510 Å), B (4390 Å), V (5440 Å). For XRT: only WT mode data have been included, binned to 500 s; a flux of  $10^{-10}$  erg cm $^{-2}$  s $^{-1}$  is approximately equal to 3.5 – 4.5 c/s. For UVOT: U filter data are not included, since for most of the observing time the detector was saturated; for all the other filters, the flux is given in units  $10^{-14}$  erg cm $^{-2}$  s $^{-1}$  Å $^{-1}$  and is not corrected for absorption. The mark on abscissa indicates the 00 : 00 : 00 UTC of the day, i.e. the day 2035 corresponds to 29 July 2006 at 00 : 00 : 00.

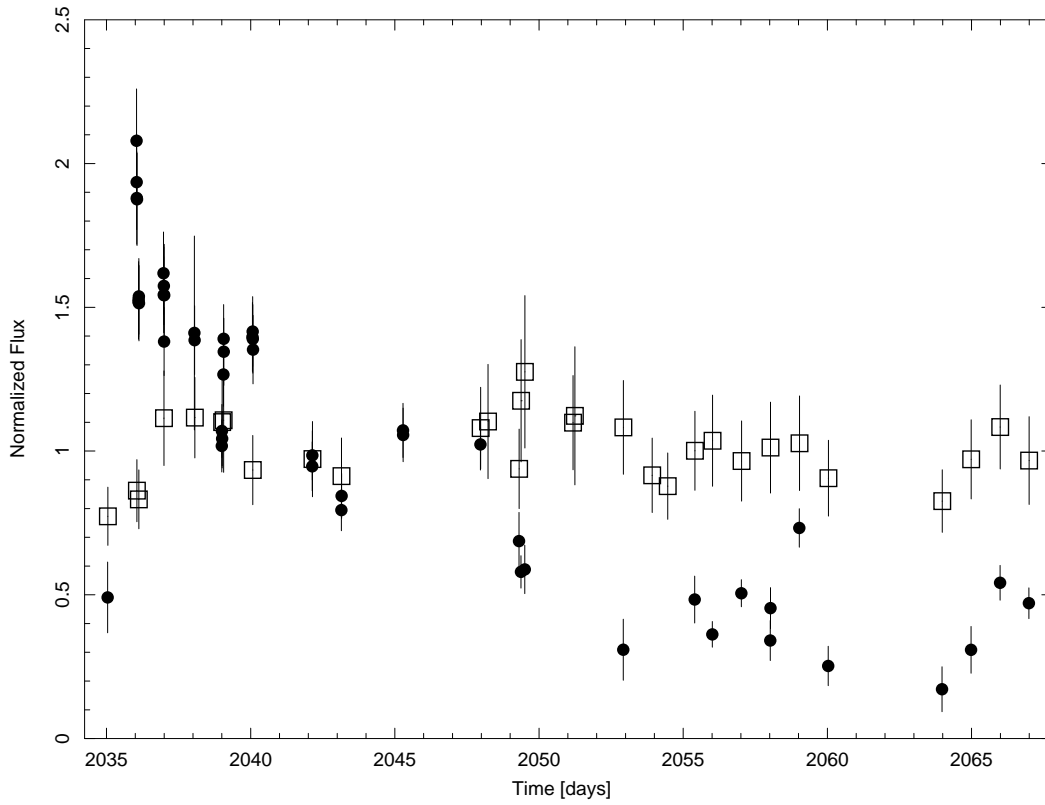


Fig. 2.— Normalized lightcurves. Black filled circles indicate XRT data [0.3 – 10 keV] normalized to their average in July-August 2006 ( $7.1 \pm 0.6$  c/s). Open squares indicate the average from UV filters, which are UVW2 (1880 Å), UVM2 (2170 Å), and UVW1 (2510 Å), normalized to  $(11.6 \pm 0.6) \times 10^{-14}$  erg cm $^{-2}$  s $^{-1}$  Å $^{-1}$ .

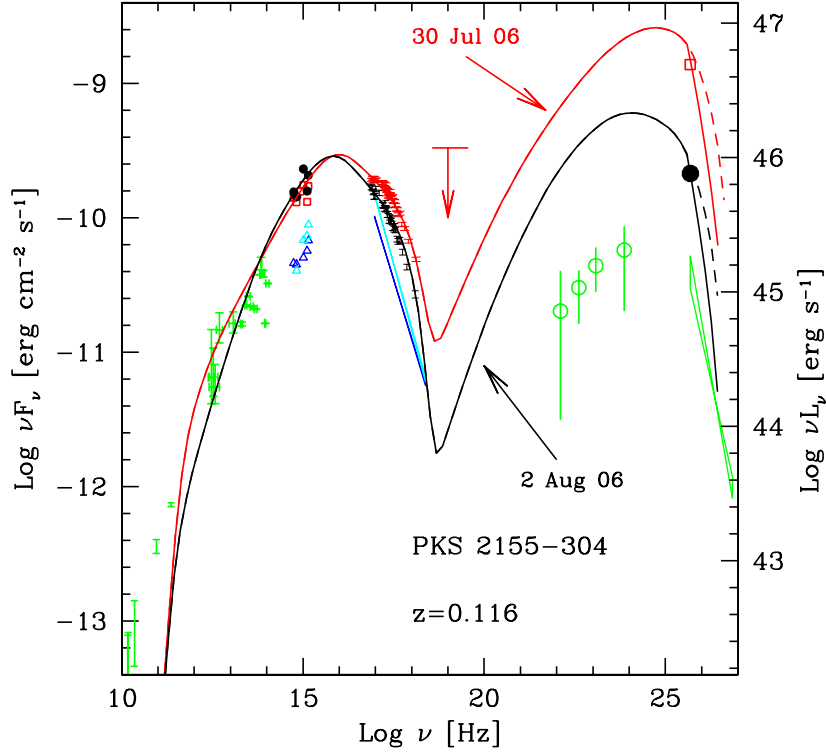


Fig. 3.— Spectral Energy Distribution of PKS 2155–304: the red symbols are the quasi-simultaneous data of 29 July; the black symbols refer to the observations of 2 August. HESS data from Raue et al. 2006; *Swift* quasi-simultaneous data are from the present work. For comparison, we also report data from the historical records: green symbols refer to archival data (references in Chiappetti et al. 1999) and to the H.E.S.S. TeV spectrum taken in October–November 2003 (Aharonian et al. 2005b), while other colors report the *XMM-Newton* data from Foschini et al. (2006). The red continuous line represents the synchrotron self Compton model (SSC, see Ghisellini et al. 2002) used to fit the data of 29 July 2006, while the black line represents the model fitted to the data of 2 August. Both models include the absorption at TeV energies due to the extragalactic infrared background calculated according to Stecker & Scully (2006). The dashed line indicates the intrinsic (i.e. not absorbed) spectrum.